Journal of Metallurgy and Materials Science, Vol. 63, No. 3-4, July-December 2021
Printed in India, © NML, ISSN 0972-4257

Effect of Uniaxial Tensile Strain and Heat Treatment on Corrosion Behavior of AISI 304 Stainless Steel

SUJIT KUMAR GUCHHAIT *, SHAMPA DHAR, P. K.MITRA
Metallurgical and Material Engineering Department, Jadavpur University, Kolkata-700032, India

Abstract : In this present study, we are attempted to correlate the corrosion behavior of AISI 304 stainless steel (SS) caused by the microstructural changes occurring due to the combined effect of different degrees of uniaxial tensile strain and heat treatment. For this purpose, AISI SS304 samples were prior deformed uniaxially from 10% to 50%. The deformed portion was cut to small rectangular pieces and heat-treated at a temperature of 600^0C for 1 hr in Vaccum (air pressure ~ 10^{-3}mbar). This study reveals that corrosion resistance property has been significantly changed with deformation and sensitized temperature as compare to deformed unsensitized stainless steel. XRD, SEM and hardness testing were carried out to understand the microstructural changes. Potentiodynamic polarization and EIS study were done to characterize the corrosion properties of the strained and unstrained AISI 304SS. It is noted that corrosion current (I_{corr}) increased due to the formation of chromium carbide or deformation band in the structure. Form the EIS study it is also established that polarization resistance at 600 °C temperature and deformation decreased due to formation of tempered martensite along with carbide precipitation.

Keywords : *AISI 304 stainless steel, Tensile strain, Heat treatment, XRD, polarization study, EIS*

1. INTRODUCTION:

Austenitic stainless steel (SS) is the backbone of the modern industry since it finds a huge application in nuclear, chemical, petrochemical, power generation allied industry due to its high ductility, excellent mechanical strength, and corrosion resistance properties [1]. The high chromium (Cr) percent (> 12 %) in these alloys plays an important role to achieve enhanced resistant properties against various uniform corrosions [1-3]. The major drawback related to these steels is their vulnerability to intergranular corrosion (IGC) because of sensitization [4]. The sensitization process involves the precipitation of chromium carbides and the depletion of chromium in the grain boundaries when steel is subjected to heat or slowly cool during the temperature range 1123K to 723K [5 – 13]. The sensitization process depends on several factors like; heating temperature heating, chemical composition, time [5, 14 -16]. Several studies are revealed sensitization can also be influenced by prior deformation or strain [17- 27]. Kain, et al. reported that 304, 304L and 304LN grade SS developed martensite phase after 15% cold working which led to sensitize at 500 ^{0}C temperature [28]. Singh et al. showed that cold deformation improved the degree of sensitization as high as 65 times the undeformed AISI 304 at 500^0C [29]. They are also suggested that with increasing deformation; the carbide precipitation takes place at the grain boundary region. Atanda et al. are observed that SS316L was sensitized when heated to 750 – 850 ^{0}C for 0.5 – 2 hrs before normalizing[30]. Recently, Zhang et al have investigated the effects of pre-strain (up to 20 %) on the degree of sensitization (DOS) and IGC of 304 SS which was thermally aged at 750 °C for one hour [31]. The study revealed that the degree of sensitization and the susceptibility to IGC are proportional to the applied pre-strain in 16 % copper-copper sulphate - sulphuric acid solution. In our early study, we have reported that DOS of 304 SS depended on the extent of deformation as well as sensitization temperatures [32]. Earlier intergranular corrosion due to cold deformation along with low temperature sensitization has been reported at comparatively higher temperature and longer ageing time [18, 29, 31]. Hence in view of the above, the present study is focused on the correlation between the corrosion behavior of AISI 304 stainless steel (SS) caused by the microstructural changes taking place owing to the combined effect of different degrees of uniaxial tensile strain and heat treatment at temperature 600 °C with

Corresponding Author :
Email: sujitguchhait.chem@gmail.com

a soaking time of 1 h. The samples were investigated by X-ray Diffraction technique (XRD), Scanning electron microscope (SEM) and Vickers hardness to understand the microstructural changes due to prior deformation and heat treatment. The electrochemical study was carried out through polarization and impedance spectroscopy in the 1N H_2SO_4 solution. It is observed that corrosion resistance property of the deformed and sensitized stainless steel samples was decreased due to formation of tempered martensite along with carbide precipitation.

2. EXPERIMENTAL

The chemical composition of the AISI 304 stainless steel (thickness 3 mm) in this present study is given in Table 1. Two tensile specimens of gauge length 30 mm each were machined and deformed at various uniaxial strain (10%, 20%, 30%, 40%, 50%) using the Instron™ tensile testing instrument at a strain rate of 10^{-3} per second. After that, the gauge length portion of the sample has been cut into five rectangular pieces. One set of samples (i.e. no strain, 10% strain, 20% strain, 30% strain, 40% strain, and 50% strain) was heat-treated at temperature 600 ^{0}C. The heat treatment was carried out under vacuum conditions(air pressure ~ 10^{-3}mbar) (Figure 1) and the soaking time was continued for 1 h followed by furnace cooling.

Table 1. Chemical composition (wt %) of AISI 304 stainless steel

C	Ni	Cr	Mn	Si	S	P	Fe
0.039	8.62	18.89	1.49	0.56	0.009	0.031	Balance

Figure 1.Vacuum-sealed (air pressure ~ 10^{-3} mbar) AISI 304 samples

2.1. Material Characterization:

1The XRD analysis of all the samples was performed by Rigaku X-Ray Diffractometer, Ultima III using Cu Kα (0.154056 nm) radiation in the 2 theta range 30° to 80°. The microstructural analysis of each sample was investigated with scanning electron microscopy (SEM, JEOL JSM-6360). Before microstructural analysis, all the samples were polished with different grade emery papers and washed in DI water then etched by10 % HNO_3 + 30 % HCl + 60 % DI water solution. The hardness of the investigated samples of AISI 304 austenitic stainless was taken in Vicker's hardness tester. The hardness measurements were done using a load value of 30 kg for 5 sec.

2.2. *Electrochemical Characterization:*

Electrochemical studies were done using a standard three-electrode system by Gamry Instrument at room temperature using a 1NH_2SO_4 solution. For the electrochemical measurement, graphite rod and saturated calomel electrode (SCE) were used as counter electrode and reference electrode respectively. The deformed and sensitized AISI 304 samples were used as a working electrode. Prior to each experimental performance, the working electrodes were polished with emery paper progressively up to 2/0 and finally polished by cloth, then degreased with alcohol and washed with running distilled water twice. Potentio dynamic polarization studies of the samples were performed with a scan rate of 1 mV/s in the 1N H_2SO_4 solution. Electrochemical Impedance Spectroscopy

(EIS) study was also carried out in the same instrument in a frequency range from 0.01 Hz up to 100 kHz at 10 mV amplitude in 1N H_2SO_4 solution. Here all electrochemical curves were analyzed by Echem Analyst software and all potentials are reported with respect to SCE.

3. RESULTS AND DISCUSSION:

Figure 2 (a - b) shows the XRD patterns of the non-heat-treated and heat-treated samples after deformation. Figure 2a compares the XRD patterns of strained and unstrained samples. It reveals that as received (unstrained and non-heat treated) sample shows the fcc (γ) phase along with the martensite phase in the matrix [32]. With increasing strain, the intensities of austenite peaks are found to gradually decrease and martensite peaks appeared. However, a change is observed at a 20 % strained sample where α' (110) peaks are vanishing due to the preferred orientation [32]. However,α' (110) peaks re-appears at 30 % strain and intensity gradually increases with the percentage of strain. This deformation-induced martensite(DIM) during tensile deformation may be due to stacking fault energy of AISI 304 SS [29]. At higher temperature, at 600 ^{0}C, α' martensites present in all diffractograms (Figure 2b) and it beg into transform into tempered martensite(α + $M_{23}C_6$) having carbide precipitation results in the phase mixture of α and α' [32]. Therefore, at a higher,temperature, a significant enhancement in the peak intensity adjacent to the (111) γ peak is observed.

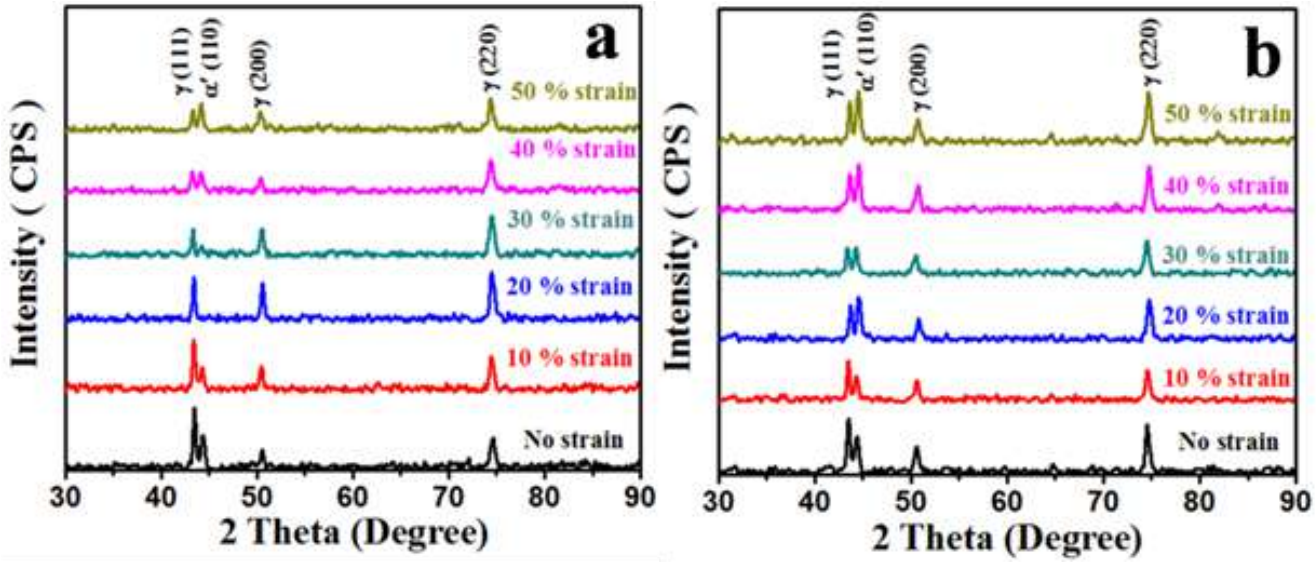

Figure 2. XRD analysis (a) non-heat-treated (b) heat-treated at 600 ^{0}C samples at different strain

Figure 3 (a – f) and Figure 4 (a – f) shows the Scanning Electron Micrographs (SEM) of strained and unstrained samples. Figure 3a reveals that little amount of deformation band is present in the unstrained non heated sample. It was found that with increasing strain significant microstructural change is observed. Populations of deformation bands are predominantly starting forming from 20 % strain (Figure 3(b – f)). Hence it is worth mentioning that, at the grain boundary region, these deformation bands can act as the energetically favorable zone for the precipitation of chromium carbide, resulting in the formation of depletion regions in the near band zones. It is noted that with increasing temperature (600 ^{0}C) these deformation bands are clearly observed (Figure4 (a – f)). Interestingly at higher strain and temperature condition, chromium carbide precipitation took place along the grain boundary and deformation band region are also significantly prominent in the micrographs. It is also being noted that carbide precipitation is a time temperature-dependent process that is determined mostly by carbon diffusion at low temperatures and carbide solubility at elevated temperatures [33].

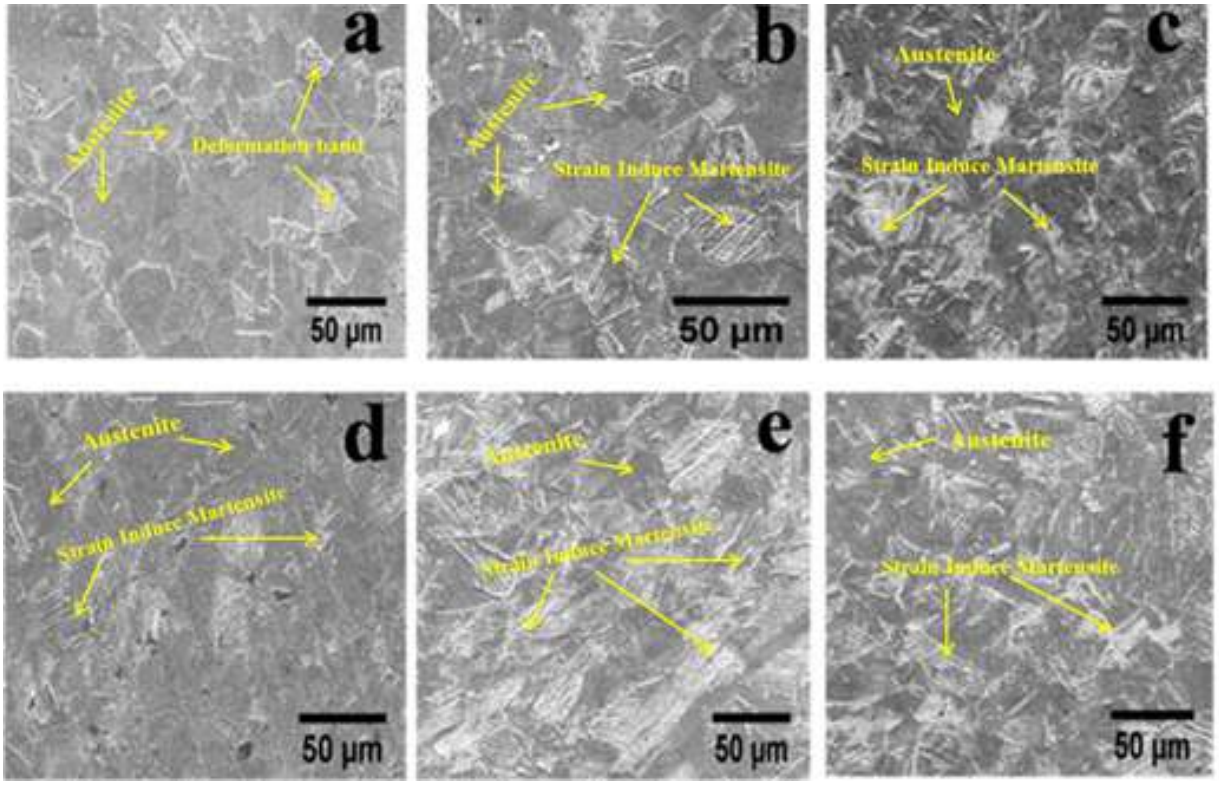

Figure 3.SEM micrographs of non-heat-treated samples (a) un-strain (b) 10% strain (c) 20 % strain (d) 30% strain (e) 40 % strain (f) 50% strain

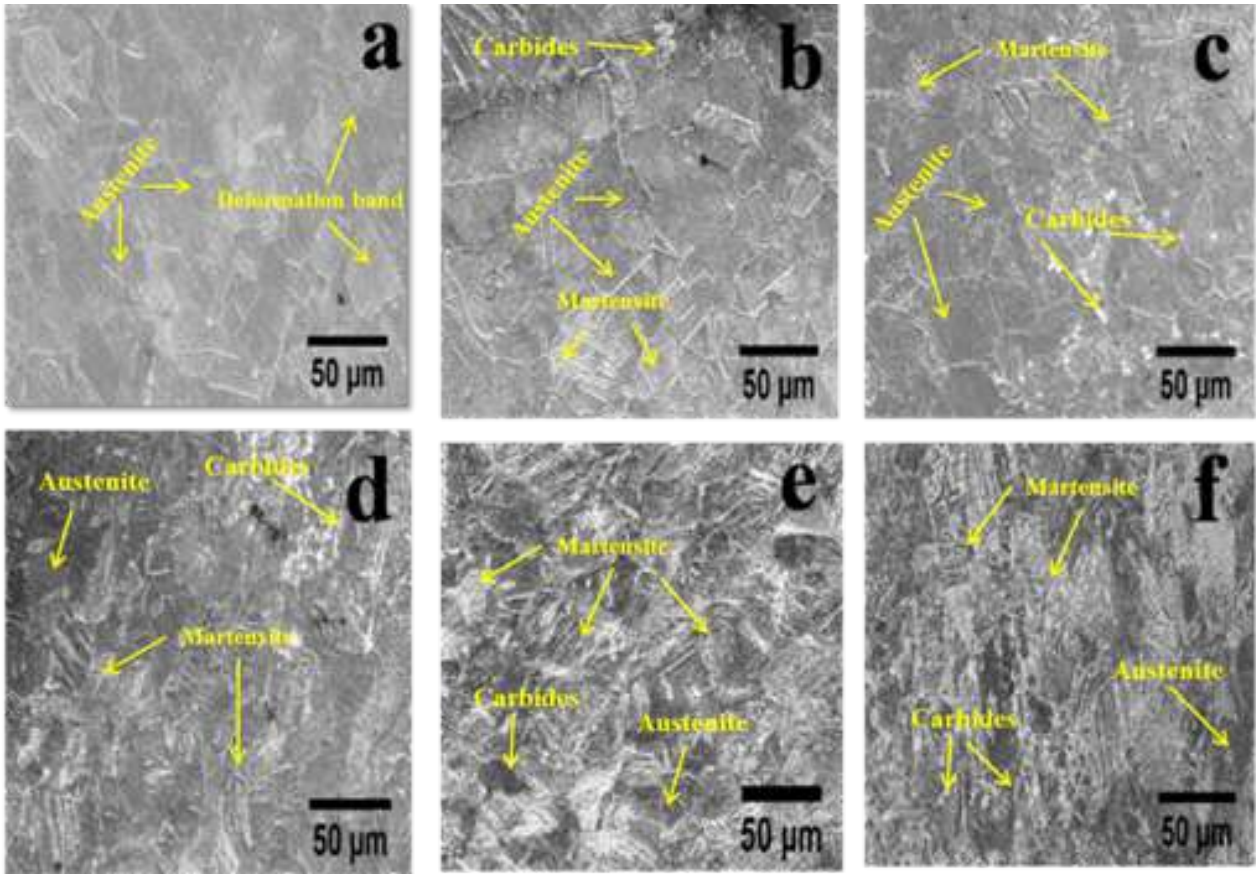

Figure 4.SEM micrographs of 600 ^{0}C heat treat samples (a) unstrain (b) 10% strain (c) 20 % strain (d) 30% strain (e) 40 % strain (f) 50% strain

Vicker's hardness of the samples is given in Figure 5. From XRD and SEM study it was revealed that as received sample contains fcc (γ) phase along with martensite and with increasing strain SIM formation takes place (except 20 % strain). It is reported that the martensite phase is harder than the ferrite or austenite phase [34]. Hence, the hardness of non-heat-treated samples increases with increasing strain. In the case of 600 ^{0}Cheat-treated samples, the hardness of 10% deformed sample decreases as compared to the unstrained sample which may be due to stress relaxation. Nevertheless, after that hardness value increases upto 30 % deformed which is may be due to the formation of martensite phases along with and carbide precipitation (supported by XRD and SEM study) along the grain boundaries. Although hardness value again decreases at higher deformation because of carbon diffused toward grain boundary along with the martensite phase is starting disappearing from the microstructures.

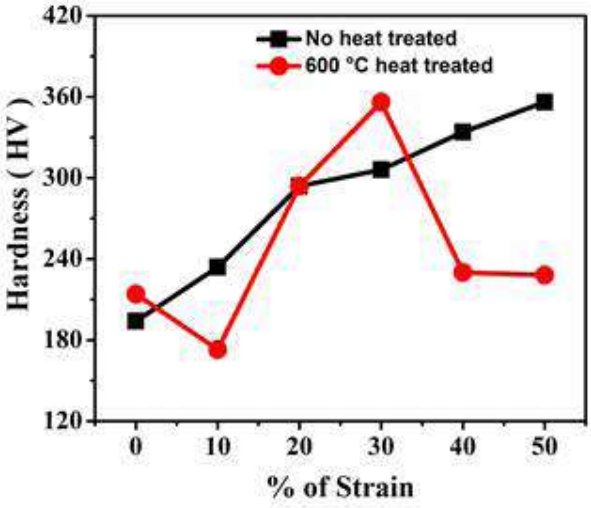

Figure 5.Vickers hardness of the non-heat treated and heat-treated samples

A comparative polarization curve of the non-heat treated unstrained and strained samples in 1 N H_2SO_4 solution is given in Figure 6a. It is found that the corrosion current (I_{corr}) of the as-received unstrain sample is 3.7 μA/cm^2 which gradually decreases upto 20 % strained samples (I_{corr} = 0.31 μA/cm^2) due to suppression of (111) α' phase as discussed in the previous section.

However after that, with increasing strain, corrosion current enhances due to DIM and 50 % strained sample attained maximum Icorr (I_{corr} = 564.5 μA/cm^2) (Table 2). A comparison curve of 600 ^{0}Cheat-treated samples is shown in Figure 6b. 600 ^{0}Cheat-treated samples show reduced Icorr up to 30% strained sample (Table 2). After 30% of deformation I_{corr} increases which is due to the precipitation of chromium carbide at higher deformation and temperature. From Figure 6 (a – b) it is also revealed that deformed non-heat-treated samples give superior nobler properties than deformed 600 °C heat-treated samples (Table 2).

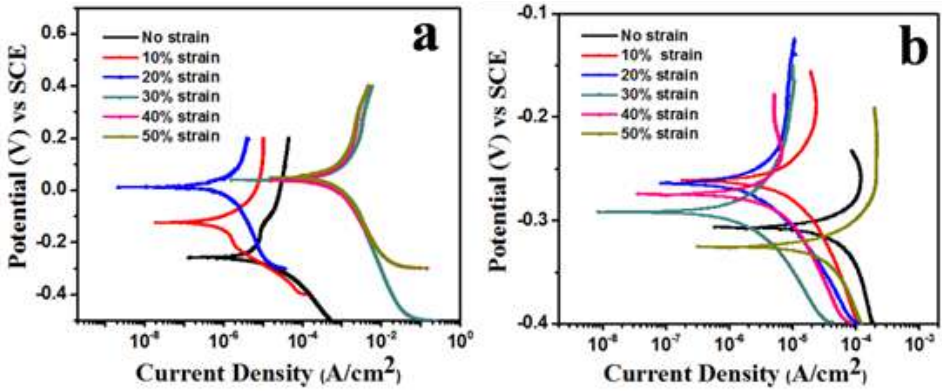

Figure 6.Potentiodynamic polarization study of (a) non-heat-treated (b) heat-treated at 600 ^{0}C samples at different strain

Table 2. Polarization data of the non-heat-treated and heat-treated samples at different strain

Sample	I_{corr} (μA/cm²)		E_{corr} (mV vs. SCE)	
	No Heat	At 600 ^{0}CHeated	No Heat	At 600 ^{0}CHeated
No Strain	3.7	36.2	-260.5	-308.9
10% Strain	0.87	6.1	-127.6	-265.0
20% Strain	0.31	2.2	14.8	-265.0
30% Strain	545.2	1.1	20.8	-293.5
40% Strain	548.4	3.1	25.2	-269.7
50% Strain	564.5	38.8	34.1	-334.7

Electrochemical Impedance Spectroscopy (EIS) studies were done for a better understanding of the fundamental feature of electrochemical behavior at the electrolyte - metal interface. The electrochemical process at the surface is a complex phenomenon, which consists of different ions interactions, polarization resistance (R_p), impedance and other parameters due to interaction between electrolyte and electrode. The overall process can be summarized by an equivalent AC electrical circuit which is depicted and discussed in this section. The EIS spectra of all the samples are shown in Figure 7 (a – b) and the EIS data are tabulated in Table 3. All the spectra were fitted in the constant phase element model (CPE) (Figure. 8a) except non-heat-treated samples of 30 %, 40 % and 50 % strained samples. These are fitted in CPE with diffusion model (Figure 8b). Mathematically, simple CPE model can be expressed by:

$$Z_{CPE} = \frac{1}{Y_0(j\omega)\alpha}$$

Where j represents the imaginary function, ω is the angular frequency, Y_0 is CPE constant, α is an exponent of constant phase element ranging from 0 to 1. A high α value is typically for the material which has a strong capacitive nature. A higher polarization resistance (R_p) implies greater corrosion resistance of the material in a given environment. Figure 7a shows the Nyquist plot of the non-heat-treated samples. From these curves, it is clear that un-strained, 10% and 20% strained samples tend to become semicircle. It is found that with increasing strain (upto 20 %) polarization resistance (R_p) increases however after that R_p decreases with deformation due to an increase of DIM in the matrix(Table 3). On the other hand, 600^{0}C heat treatment samples also tend to form semi-circle shows in the Nyquist plot. From Figure 7 (a – b) it is clearly revealed that increasing stain and temperature corrosion resistance properties deteriorated as compared to the non-heat-treated samples due to the formation of carbide precipitation.

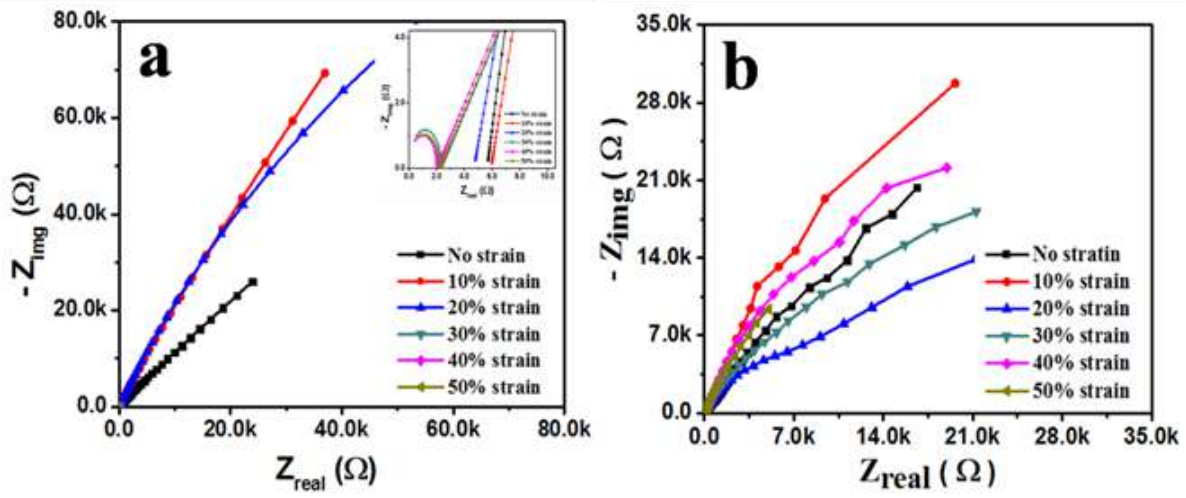

Figure 7.Nyquist plot of (a) nonheat-treated (b)600 ^{0}Cheat-treated samples at different strain

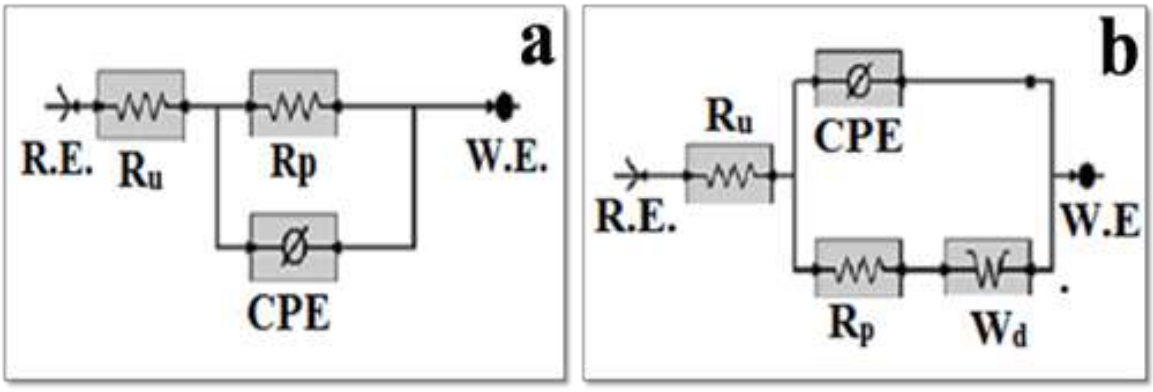

Figure8: Equivalent model circuit for (a) CPE; (b) CPE with diffusion model where, R_u = Solution resistance, CPE = Constant phase element, R_p= Polarization resistance, W_d = Warburg element

Table 3: Electrochemical impedance data of all the samples

Sample	R_u ohms (Ω)		$R_p$ohms (KΩ)		Y_0 ($\times 10^{-6}$) (S*s^a)		A		Wd (S*s^1/2)	
	No Heat	600 °C Heated	No Heat	600 °C Heated	No Heat	600 °C Heated	No Heat	600 °C Heated	No Heat	600 °C Heated
No Strain	4.5	3.2	27.6	60.80	91.85	73.5	0.68	0.73	-	-
10 % strain	5.8	5.3	376.4	326.1	93.12	86.7	0.75	0.74	-	-
20 % strain	4.6	3.4	445.9	27.72	70.56	110.5	0.75	0.73	-	-
30 % strain	0.3×10^{-3}	1.7	0.002	55.20	0.36	86.07	0.95	0.75	0.18	-
40 % strain	0.1×10^{-3}	3.1	0.0019	88.03	0.48	102.4	0.91	0.77	0.24	-
50 % strain	0.8×10^{-3}	2.4	0.0022	87.79	0.8	106.2	0.93	0.76	0.22	-

4. CONCLUSIONS:

From the above results and discussion; a correlation between the corrosion behavior of AISI 304 SS caused by the microstructural changes taking place due to the combined effect of different degrees of uniaxial tensile strain (10 %, 20 %, 30%, 40 %, and 50%) and heat treatment is established. So in conclusion,

a. AISI 304 stainless steel significantly influenced by uni-axial tensile stain and sensitization temperature. The SEM micrographs obtained from the strained and heat-treated samples showed the existence of deformation bands in all the samples. At higher strain and temperature, chromium carbide precipitations along the grain boundary and deformation band region are also significantly prominent.

b. The corrosion resistance properties and solution resistance properties of sensitized and un-sensitized samples are notably affected by marten site and carbide phases. At higher deformation (50 %) and higher heat treatment temperatures complex microstructural changes cause opposing corrosion behavior in the sample. In 1 N H_2SO_4 solution, deformed non-heat-treated samples give superior nobler properties than deformed 600 °C heat-treated samples.

ACKNOWLEDGMENTS

The authors would like to Jadavpur University, Kolkata to carry out this research work. SKG also thanks to Dr. Paramita Mukherjee, Dr. N. Gayathri Bannerjee of Variable Energy Cyclotron Centre (VECC), Kolkata and Dr. P. S. Chowdhury of Jadavpur University, who gives their valuable suggestion for conducting heat-treatment process and material problems.

REFERENCES

[1] G. George, H. Shaikh: 1-Introduction to austenitic stainless steels, Corrosion of austenitic stainless steels, Wood head Publishing, pp1-36, 2002

[2] V. G. Rivlin, G. V. Raynor: 1: Critical evaluation of constitution of chromium-iron-nickel system, Int. Met. Rev. 25, 21-40, 1980

[3] V. P. Kujanpaa, N.Suutala,T. Takalo, T. Moisio: Correlation between solidification cracking and microstructure in austenitic and austenitic-ferritic stainless steel welds, Weld.Res. Inter.,9, 55-75, 1979

[4] C.S. Tedmon, D.A.Vermilyea, J.H. Rosolowski: Intergranular corrosion of austenitic stainless steel, J. Electrochem Soc., 118, 192-202, 1971

[5] R.T. Holt, W. Wallace: Impurities and trace elements in nickel - base super alloys, Int. Met. Rev. 21(1), 1-24, 1976

[6] X. Huang, H. Wang, W. Xue, S. Xiang, H. Huang, L. Meng, G. Ma, A.Ullah, G. Zhang: Study on time-temperature-transformation diagrams of stainless steel using machine-learning approach, Comput. Mater. Sci. 171, 109282, 2020

[7] D. Özyürek: An effect of weld current and weld atmosphere on the resistance spot weld ability of 304L austenitic stainless steel, Mater. Design.29, 597-603, 2008

[8] Z.Y. Xue, S. Zhou, X.C. Wei: Influence of pre-transformed marten site on work-hardening behavior of SUS 304 metastable austenitic stainless steel, J. Iron Steel Res. Int. 17, 51-55, 2010

[9] S. M. Tabatabaeipour, F. Honarvar: A comparative evaluation of ultrasonic testing of AISI 316L welds made by shielded metal arc welding and gas tungsten arc welding processes, J. Mater. Process. Tech., 210, 1043-1050, 2010

[10] P. M. Silva, H.F. de Abreu, V.H. de Albuquerque, P. de LimaNeto, J.M. Tavares: Cold deformation effect on the microstructures and mechanical properties of AISI 301LN and 316L stainless steels, Mater. Design.32, 605-614, 2011

[11] A.J. Sedriks: Corrosion of stainless steel, 2 ed., United States, N. P., Web, 1996

[12] V. Cihal, Intergranular Corrosion of Steels and Alloys, Elsevier, Amsterdam, 1994

[13] A.S. Lima, A.M. Nascimento, H.F. Abreu, N. P. de Lima: Sensitization evaluation of the austenitic stainless steel AISI 304L, 316L, 321 and 347, J. Mate. Sci., 40, 139-144, 2005

[14] M.D. Mathew, G. Sasikala, K.B. Rao, S.L. Mannan: Influence of carbon and nitrogen on the creep properties of type 316 stainless steel at 873 K, Mater.Sci. Eng.A, 148, 253-260, 1991

[15] M. Stalder, S.Vogel, M.A. Bourke, J.G. Maldonado, D.J. Thoma, V.W.Yuan: Retransformation ($\alpha' \rightarrow \gamma$) kinetics of strain induced marten site in 304 stainless steel, Mater. Sci. Eng. A, 280, 270-281, 2000

[16] R. Beltran, J.G. Maldonado, L.E. Murr, W.W. Fisher: Effects of strain and grain size on carbide precipitation and corrosion sensitization behavior in 304 stainless steel, Acta Mater., 45, 4351-4360, 1997

[17] K.H. Lo, D. Zeng, C.T. Kwok: Effects of sensitisation-induced martensitic transformation on the tensile behavior of 304 austenitic stainless steel. Mater.Sci. Eng.A, 528, 1003-1007, 2011

[18] C. S. TedmonJr, D.A. Vermilyea, D.E. Broecker: Technical note Effect of cold work on intergranular corrosion of sensitized stainless steel, Corrosion., 27, 104-106, 1971

[19] H.D. Solomon, The influence of prior deformation on continuous cooling sensitization of type 304 stainless steel, Corrosion., 36, 356-661, 1980

[20] S. Pednekar, S. Smialowska: The effect of prior cold work on the degree of sensitization in type 304 stainless steel, Corrosion., 36, 565-577, 1980

[21] H.D. Solomon, D.C. Lord: Influence of strain during cooling on the sensitization of type 304 stainless steel, Corrosion., 36, 395-399, 1980

[22] C.L. Briant, A.M. Ritter: The effect of marten site on the sensitization of low carbon 304 stainless steel, Metal. Trans. A.,12(5), 910-913, 1981

[23] M.J. Povich, D.E. Broecker : Stress corrosion cracking of austenitic stainless steel alloys in high-temperature air-saturated water, Mater. Perform.,18, 41-48, 1979

[24] S. Pednekar, S. Smialowska: TheEffect of Prior Cold Work on the Degree of Sensitization in Type 304 Stainless Steel, Corrosion., 36, 565-577, 1980

[25] K.A. Johnson, L.E.Murr, K.P. Staudhammer: Comparison of residual microstructures for 304 stainless steel shock loaded in plane and cylindrical geometries: implications for dynamic compaction and forming, Acta Metall., 33, 677-684, 1985

[26] E. Almanza, L.E. Murr: A comparison of sensitization kinetics in 304 and 316 stainless steel, J. Mater. Sci., 35, 3181–3188, 2000

[27] C.L. Briant, A.M. Ritter: The effect of gold work on the sensitization of 304 stainless steel, Scr Metall., 13, 177-181, 1979

[28] V. Kain, K. Chandra, K.N. Adhe, P.K. De: Effect of cold work on low-temperature sensitization behaviour of austenitic stainless steels, J. Nucl. Mater., 334, 115-132, 2004

[29] R. Singh: Influence of cold rolling on sensitization and intergranular stress corrosion cracking of AISI 304 aged at 500° C, J. Mater. Process. Tech., 206, 286-293, 2008

[30] P. Atanda, A. Fatudimu, O.Oluwole: Sensitisation Study of Normalized 316L Stainless Steel, J. Miner. Mater. Char. Eng., 9, 13-23, 2010

[31] X. Zhang, J. Tang, H. Liu, J. Gong: Effects of pre-strain on sensitization and interganular corrosion for 304 stainless steel, Eng. Fail. Anal., 106, 104179, 2019

[32] P.S. Chowdhury, S.K. Guchhait, P.K.Mitra, P. Mukherjee, N.Gayathri,M.K.Mitra: Understanding the effect of uniaxial tensile strain on the early stages of sensitization in AISI 304 austenitic stainless steel, Mater. Chem. Phys., 155, 217-222, 2015

[33] R.K. Dayal, J.B. Gnanamoorthy: Predicting extent of sensitization during continuous cooling from TTS diagram, Corrosion., 36, 104-106, 1980

[34] J. Mola, M. Ren:on the hardness of high carbon ferrous martensite, IOP Conf. Ser.: Mater. Sci. Eng.,373, 012004, 2018